JOURNAL OF APPLIED ELECTROCHEMISTRY 23 (1993) 358–363

Hydrogen permeation during zinc–manganese alloy plating

K. N. SRINIVASAN, M. SELVAM, S. VENKATA KRISHNA IYER

Central Electrochemical Research Institute, Karaikudi 623 006, Tamil Nadu, India

Received 6 May 1992; revised 2 September 1992

Electrodeposition of metals from solution is usually accompanied by the simultaneous discharge of hydrogen ions or water molecules. When hydrogen is liberated at an iron/steel surface during electrodeposition, a portion of the hydrogen is absorbed by the metal surface and then diffuses into the interior. The diffused hydrogen produces some detrimental effects, such as reduction in ductility and loss in mechanical strength, leading to hydrogen embrittlement. The present paper reports investigations on hydrogen permeation measurements in zinc–manganese alloy deposition using a modified electrode clamp for easy removal and fixing of the electrode. Hydrogen permeation studies indicate that the porosity of the deposit increases in the following order:

Zn–Mn(14.3%), Zn–Mn(2.4%), Zn–Mn(24.8%) and Zn–Mn(37.5%).

This is in agreement with the corrosion data obtained which indicates that Zn–Mn alloy deposits with low manganese content show better performance than pure zinc deposits.

1. Introduction

Metallic coatings of nickel, copper and zinc have been generally used for the protection of mild steel. Zinc and its alloys are widely used as anode materials for the cathodic protection of steel structures. The standard electrode potential of manganese is more negative than that for zinc so that it can protect steel structures against corrosion more effectively than zinc [1, 2]. But manganese has not been considered as a protective coating for steel because of the assumption that its chemical reactivity is relatively severe in all media and also because of its brittle nature. Manganese films may become tarnished with a brown film immediately after deposition, so that manganese cannot be used as a coating when appearance is of prime importance. Moreover tarnished films or corroded coatings are very similar to the corrosion products of iron. The corrosion resistance, as well as the appearance, of the manganese coating can be improved by codepositing it with other metals such as iron, nickel, copper, zinc, chromium, cobalt etc. A few patents and papers [3–6] have claimed that corrosion resistant coatings of zinc–manganese alloys may be produced from aqueous baths. Deposition of zinc and its alloys is usually carried out on steel surfaces.

There has been renewed interest in studies on hydrogen absorption and hydrogen embrittlement of steel. Metal deposition is usually accompanied by the simultaneous discharge of hydrogen ion or water molecules [7–10]. When hydrogen is liberated on an iron/steel surface during deposition a certain amount of the hydrogen is absorbed by the metal surface and diffuses into the interior of the steel. Most probably hydrogen may be liberated to some extent in the atomic state and it is absorbed only in this form. The diffused hydrogen produces some detrimental effects [11] on the mechanical properties of iron/steel, such as reduction in the ductility and loss in mechanical strength leading to hydrogen embrittlement.

Of the various techniques available for measuring the amount of hydrogen permeated through the mild steel membrane, the technique developed by Devanathan and Stachurski [8] is the simplest and most accurate. The cell used by these workers consists of two glass compartments separated by a steel membrane. The steel membrane is sandwiched between two Teflon bushings attached to the steel. This arrangement gives rise to the following problems:

(i) For each experiment bolts and nuts have to be loosened fully for removal and insertion of the steel specimens.

(ii) During tightening the alignment of the two Teflon bushings are affected. This gives rise to the problem of escape of hydrogen through the sides of the membrane.

The present study deals with the design aspects of a new clamp used for electropermeation studies, and also permeation current measurements, carried out using this clamp in zinc–manganese alloy plating baths at various current densities. Corrosion studies were also carried out using galvanostatic polarisation and weight loss measurements and the results are discussed.

2. Experiments

2.1. *Design of the clamp for fixing the metal membrane*

Figure 1 shows the mounting arrangement of the steel specimens with Teflon bushings, bolts and nuts used

0021-891X

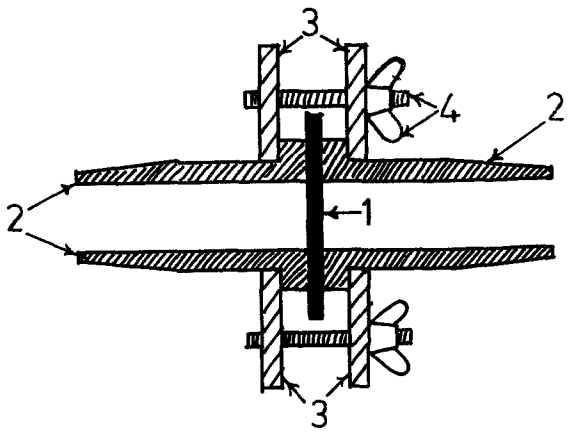

Fig. 1. Mounting arrangement. (1) Steel membrane, (2) Teflon bushings, (3) steel frame, and (4) steel nuts and bolts.

by previous workers [12–23]. Figure 2a and b represent the new PVC discs A and B. A round disc (A), with a concentric round hole, carries the Teflon bushing which tightly fits the ground glass joint of one compartment of the cell. The outer rim of the disc is knurled for easy handling. Another round PVC disc (B) with a concentric round hole takes in the other Teflon bushing fitting the ground glass joint of the second compartment. A rectangular slot is cut in the inside face of the disc as shown in the figure with width equal to the width of the membrane. Disc A has an internal thread and disc B has an external thread; when disc B is screwed into disc A, with the Teflon bushings in position, a gas-tight and water-tight seal is obtained. By unscrewing B slightly, an opening is created between the bushings through which the iron membrane is inserted and the discs are tightened by screwing. Figure 3 shows the arrangement of the membrane in position. Figures 4 and 5 show the cross section of the cell separately and the membrane in position.

2.2. *Hydrogen permeation studies in Zn–Mn alloy plating bath*

Mild steel specimens of composition C(0.063%), Mn(0.23%), S(0.03%), P(0.011%) and Fe balance were used for this study. Specimens of size 2.5 cm × 5 cm were polished and degreased; one side of the specimen was masked with lacquer and the other side was plated with palladium in the following manner: 100 ml of double distilled water was heated to 80 °C and 1 g dm^{-3} of palladium chloride was added

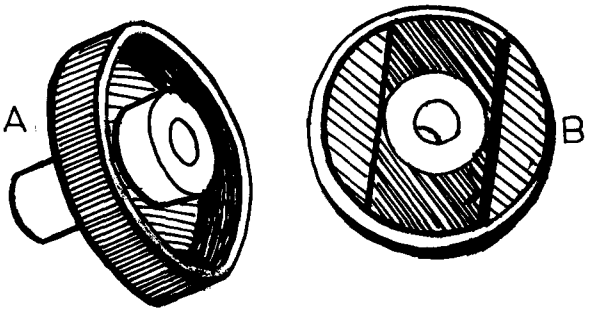

Fig. 2. PVC discs A and B with Teflon bushings.

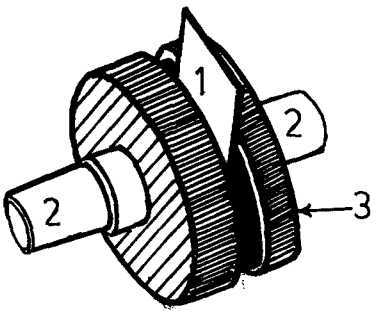

Fig. 3. Arrangement of membrane in position with PVC clamp. (1) Steel membrane, (2) Teflon bushings, and (3) PVC coupling.

followed by sodium nitrite to obtain a clear solution. Plating was carried out at 100 $\mu A\,C\,m^{-2}$ for 90 min using platinum as the auxiliary electrode. Then the specimen was washed well with tap and distilled water and then the lacquer was removed.

The membrane was then inserted in the clamp and screwed tightly. The two compartments were fitted as in the set up (Fig. 6). The anode compartment was filled with 0.2 M NaOH which was preelectrolysed and deaerated using nitrogen. A potential of −300 mV with respect to Hg/HgO/0.2 M NaOH was impressed between the reference electrode and the working electrode by means of potentiostat (Wenking Model POS 73). Water was circulated through the double wall of the cell and the temperature was maintained at 30 ± 2 °C. The potential was maintained steady and constant until a steady background current was obtained. In all these studies a residual current of 2–4 μA was obtained. After reaching the steady background current at the anode compartment, the Zn–Mn plating solution was introduced into the cathode compartment already maintained at a required current density using a current regulator. Experiments were carried out at different current densities. Plating

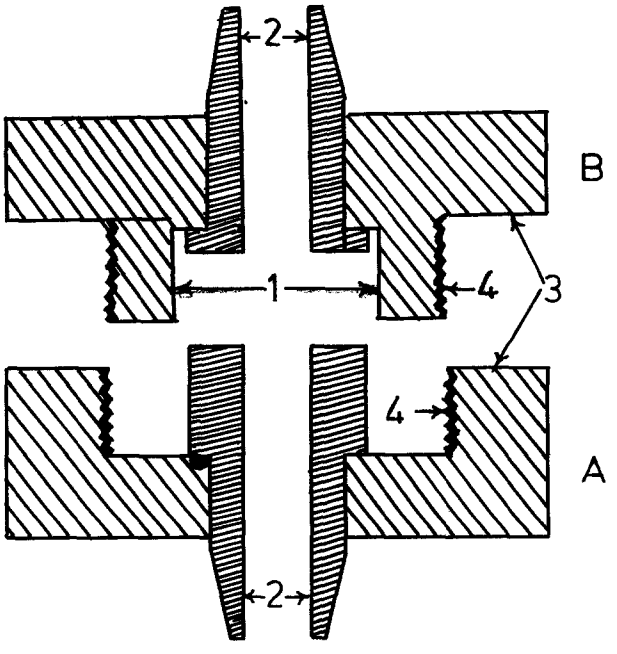

Fig. 4. Cross sectional view of the new cell showing (A) outer and (B) inner couplings. (1) Slot for steel membrane, (2) Teflon bushings, (3) PVC coupling, and (4) threaded portion.

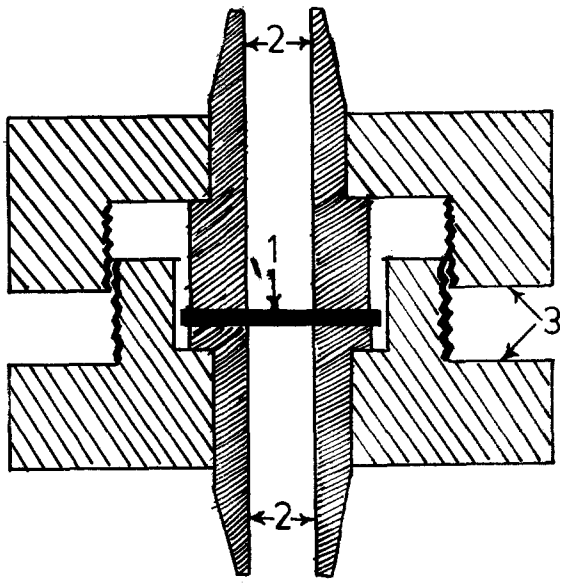

Fig. 5. Cross sectional view of the cell with steel membrane. (1) Steel membrane, (2) Teflon bushings, and (3) PVC coupling.

was carried out for 10 min and the resulting current was noted using a strip chart recorder. After the experiment the plating solution was removed immediately and the fall in current with time was recorded. Compositions and plating conditions of the plating bath are given in Table 1.

2.3. *Corrosion rate measurements*

2.3.1. *Self corrosion measurement.* Self corrosion rates of zinc containing various percentages of manganese were determined by weight loss measurements. Triplicate specimens, polished and degreased with trichloroethylene, were weighed and kept completely immersed in 200 ml of the test solution for 12 h at 30 ± 2 °C and weight loss determined.

2.3.2. *Polarization studies.* Zn–Mn alloys containing different percentages of manganese such as 2.4, 14.3, 24.8 and 37.5 plated from the bath at optimum operating conditions were used for galvanostatic polarization measurements in neutral sodium chloride solution. The auxiliary electrode was a platinum foil of area 1 cm^2. Polarization measurements were carried out after immersing the specimen for a period of 30 min, when a steady state potential was reached. Current densities in the range of 1 $\mu A\,cm^{-2}$ to 200 $mA\,cm^{-2}$ were applied and potentials vs SCE were measured after 5 min. All measurements were carried out in a thoroughly stirred electrolyte and E against $\log i$ curve was drawn. From these graphs i_{corr}, E_{corr} and corrosion rates were evaluated and are given in Table 2.

3. Results and discussion

3.1. *Hydrogen permeation studies during the deposition of Zn–Mn alloys on mild steel*

When there is no metal deposition but only hydrogen discharge at the cathode, then, after some time, the quantity of hydrogen reaching the anode becomes steady. Initially there is a steep rise in current and the shape of the current-time curve is represented in Fig. 7(a). When the metal ion starts crystallizing on the mild steel surface, the area covered by the deposit of the metal will block the entry of hydrogen. Thus, when more and more mild steel surface is covered, the quantity of hydrogen atoms reaching the anode side reaches a maximum and then declines. When the cathode side is completely covered by the deposited layer, the permeation current reduces to zero. The shape of this permeation curve is shown in Fig. 7(b) and it gives a rough indication of the nature of the surface coverage by the metal deposit, its porous characteristics and the minimum thickness of the deposit at which the deposit becomes impermeable to cathodic hydrogen. Furthermore, the total charge obtained by the integration of the curve between t_0 and t_x gives the quantity of hydrogen permeated through the composite membrane (q_H); i.e. the mild steel membrane covered with the metal deposit on the cathodic side. So if q_H is larger, the deposit will be more porous.

Hydrogen permeation curves for zinc and Zn–Mn deposits with varying manganese content are shown in Fig. 8. Values of peak permeation current (i_{max}), the time to reach peak permeation current (t_{max}), current at which no permeation and very low permeation of hydrogen occurs (i_x), the time to reach i_x, (t_x) and minimum thickness at which i_x is reached (T_{min}) are presented in Table 2. Very high values of q_H indicate

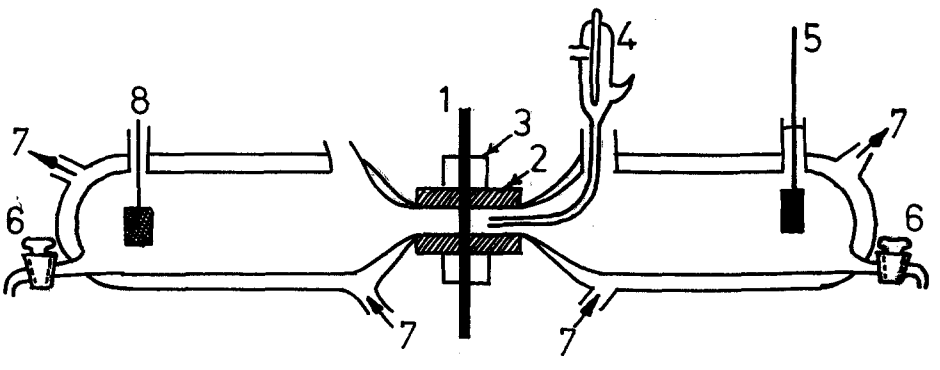

Fig. 6. Complete permeation cell setup. (1) Steel membrane, (2) Teflon bushings, (3) PVC coupling, (4) reference electrode, (5) counter electrode, (6) tap, (7) water circulation, and (8) anode.

Table 1. Zinc–manganese alloy plating bath composition and its operating conditions

Zinc sulphate heptahydrate	44 g dm^{-3}
Manganese sulphate monohydrate	61.6 g dm^{-3}
Trisodium citrate dihydrate	200 g dm^{-3}
Gelatin	0.02 g dm^{-3}
pH	5.5
Temperature	30 ± 2°C
Current density	1–8 A dm^{-2}
Deposit Mn content	2–55 wt %

that the alloy has allowed more hydrogen to pass through the membrane since the deposit is more porous. Thus, the porosity of the deposit is in the following order:

$$\text{Zn–Mn(14.3\%)} < \text{Zn–Mn(2.4\%)} < \text{Zn–Mn(24.8\%)} < \text{Zn–Mn(37.5\%)}$$

When the sites on the metal surface where hydrogen discharge is prevented by the nucleation of the metal deposit, the maximum quantity of hydrogen reaching the other side will be low and, if this coverage takes place faster, the time to reach i_{max} will be less or, for the same t_{max} values, i_{max} will be more. Thus, the steepness of the rising curve indicates the porous nature of the deposit. The metal deposit in the steady state are, therefore, arranged as Zn–Mn(14.3%), Zn–Mn(2.4%), Zn–Mn(24.8%) and Zn–Mn(37.5%) in the increasing order of porosity as per their i_{max} values in their respective permeation–time curves.

It is assumed that the decay curve represents the permeation current due to the hydrogen that is charged at pore openings still left uncovered and are being covered by the build up of metal deposits. The rate of decrease qualitatively indicates the rate of closing of the pores by the metal build up on the cathode side, as well as on the quantity of hydrogen residing on the membrane. In other words, if the time taken to reach a zero or very low permeation current is large then the deposit can be considered to be more porous. When the metal deposits are arranged in the increasing order of t_x this represents the increasing order of deposit porosity. In the present study the order is as follows:

$$\text{Zn–Mn(14.3\%)} > \text{Zn–Mn(37.5\%)} > \text{Zn–Mn(2.4\%)} > \text{Zn–Mn(24.8\%)}$$

The apparent lower porosity of the Zn–Mn(37.5%) coating than the Zn–Mn(2.4%) and Zn–Mn(24.5%) is probably due to a layer build up starting on the nucleated deposit, as well as on grain boundaries, by precipitated oxides of manganese, which may block the entry of hydrogen. The value of residual current, i_x, also indicates the probability of complete sealing of the pores by oxides.

It is interesting to note that the minimum thickness at which very low or no hydrogen permeates are 0.44 and 0.48 μm for Zn–Mn(2.4%) and Zn–Mn(14.3%) respectively, whereas it is 0.92 μm for zinc alone. This may be due to grain refinement produced by the introduction of manganese into the zinc deposit, as observed in metallographic examination.

From the overall consideration of the shape of permeation curves, it is possible to arrange the metal deposits in this study as Zn–Mn(14.3%), Zn–Mn(2.4%), Zn–Mn(24.8%) and Zn–Mn(37.5%). This agrees well with the corrosion data obtained, where it has been observed that low manganese in the deposits have shown much better corrosion resistances than pure zinc deposits.

3.2. *Corrosion studies*

Zn–Mn alloys containing different percentages of manganese such as 2.4, 14.3, 24.8 and 37.5 deposited from the bath at different current densities were subjected to corrosion studies by electrochemical methods such as weight loss measurements and Tafel extrapolation methods in 3% NaCl solutions. The corrosion data for zinc was obtained using zinc samples deposited from a bath containing zinc sulphate, sodium citrate and gelatin without manganese. The corrosion data such as i_{corr}, corrosion rate (m.p.y.: mils per year) and E_{corr} for manganese, zinc and Zn–Mn alloys are given in Table 3. It is seen from the table that all the weight losses are comparable to the corrosion rate calculated from Tafel extrapolation methods. It is also found that the alloy containing 14.3% manganese gives less corrosion rate, when

Table 2. Hydrogen permeation data

Metal deposit	$q_H/\mu C$	*Peak permeation current* I_{max}/mA	*Time to reach peak current* t_{max}/S	*Current at which very low or no hydrogen permeated* $I_x/\mu A$	*Time to reach* I_x t_x/S	*Thickness at which* I_x *is reached* $T_{min}/\mu m$
Zn	509	6.2	30	1.0	138	0.90
Zn–Mn(2.4%)	416	6.0	24	1.0	132	0.44
Zn–Mn(14.3%)	169	5.2	30	0.4	84	0.48
Zn–Mn(24.8%)	582	7.2	60	0.0	150	1.31
Zn–Mn(37.5%)	786	12.8	54	0.0	120	0.90

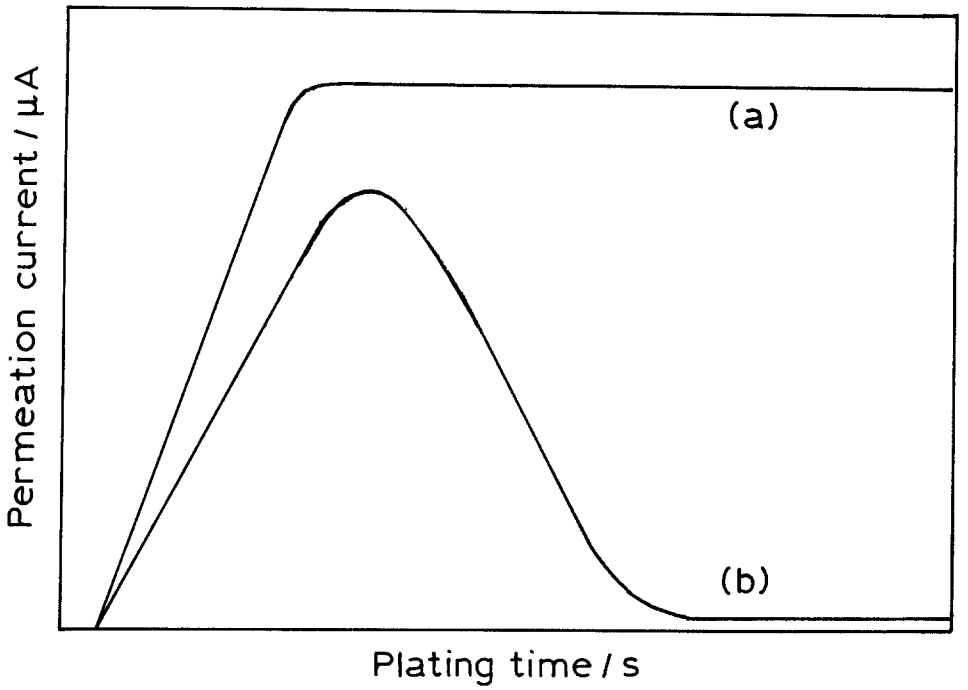

Fig. 7. Typical hydrogen permeation curves.

compared with zinc alone and other alloys of zinc and manganese. The corrosion current (i_{corr}) is also found to be less for the above alloy. This may be explained by the fact that in 3% NaCl solutions the alloy protects steel galvanically, since it has a more negative potential and a high corrosion current.

Conclusions

1. The new clamp used for hydrogen permeation measurement has the following advantages over a conventional clamp using steel bolts and nuts:
   (i) Fixing and removing the iron membrane is easier and less time consuming.
   (ii) Misalignment is completely avoided with this arrangement.
   (iii) Moreover this clamp is fabricated using PVC and Teflon and it avoids any corrosion problems arising in the clamp.
2. Zn–Mn alloy containing 2–55% manganese can be conventionally electrodeposited from the sulphate–citrate bath in the normal current density range of

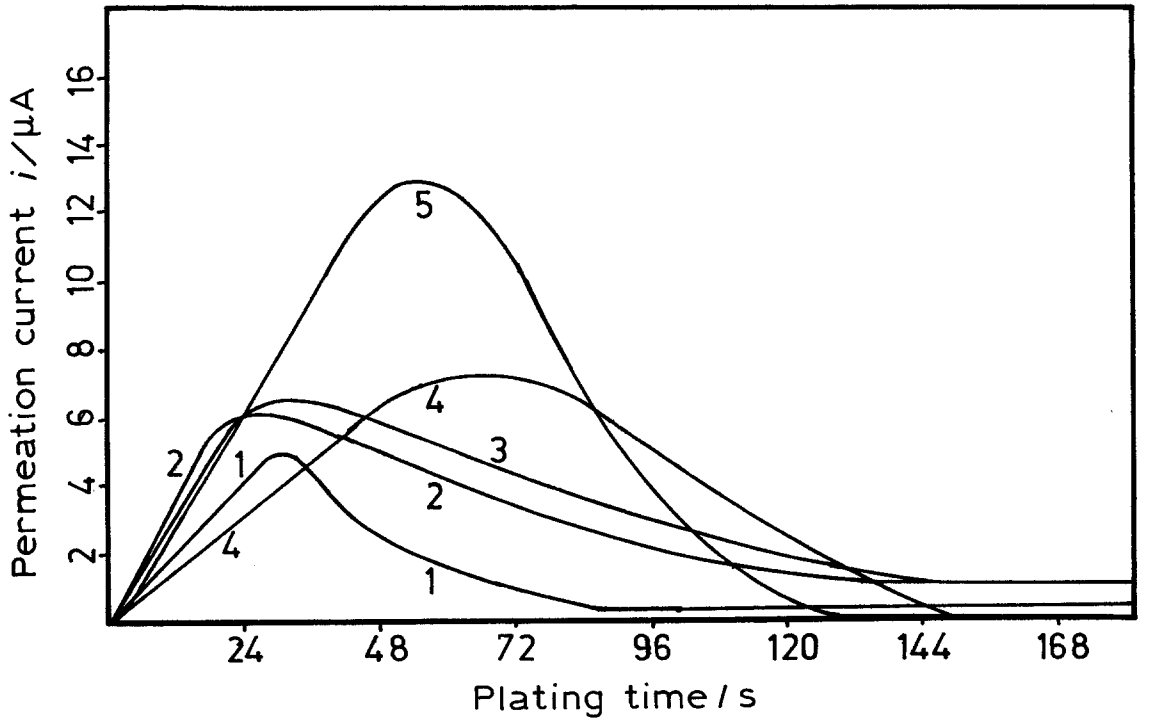

Fig. 8. Hydrogen permeation curves. Current densities, i/A dm^{-2}: (1) Zn–Mn, 2.0; (2) Zn–Mn, 1.0; (3) Zn, 2.0; (4) Zn–Mn, 4.0; (5) Zn–Mn, 6.0.

Table 3. Corrosion data for Zn–Mn alloy in 3% neutral NaCl solution

Coating	*Tafel extrapolation method*			*Corr. rate by weight loss / m.p.y.*
	E_{corr} */V(SCE)*	i_{corr} */μA cm^{-2}*	*Corr. rate /m.p.y.*	
Manganese	−1.267	175	86.8	–
Zinc	−1.035	80	47.9	50.2
Zn–Mn(2.4%)	−1.03	35	20.8	23.4
Zn–Mn(14.3%)	−1.04	26	15.1	17.8
Zn–Mn(24.8%)	−1.05	27	15.3	18.2
Zn–Mn(37.5%)	−1.05	33	18.3	21.0
Zn–Mn(54.1%)	−1.06	41	22.1	19.0

1–8 A dm^{-2} at ambient temperature and a pH of 5.5. Hydrogen permeation studies indicate that the porosity of the deposit increases in the following order:

Zn–Mn(14.3%), Zn–Mn(2.4%), Zn–Mn(24.8%)

and Zn–Mn(37.5%)

3. Zn–Mn alloy containing 14.3% manganese provides more protection than zinc of the same thickness.

References

[1] A. Brenner, 'Electrodeposition of alloys, principles and practices', Academic Press, New York (1963).
[2] M. Selvam and S. Guruviah, Proceedings of the Symposium on Industrial Metal Finishing, Karaikudi, India, July 1985, p. 225.
[3] K. K. Nippon Kokai, *Japanese patent 5 837 188* (Aug. 1981).
[4] Nippon Steel Corporation, *Japanese Patent 8 294 590* (Dec. 1980).
[5] Kawasaki, Hironobu and Watanabe Takashi, *Japanese Patent 7 735 724* (Sept. 1975).
[6] R. Sard, *Plat. Surf. Finish.* **74** (1987) 30.
[7] R. J. Barton, *Proc. Am. Electroplaters Soc.* **47** (1960) 30.
[8] M. A. V. Devanathan and Z. Stachurski, *J. Electrochem. Soc.* **111** (1964) 619.
[9] J. O'M. Bockris and D. F. A. Kioch, *J. Phys. Chem.* **65** (1961) 1941.
[10] A. N. Frumkin, *Z. Phys. Chem.* **207** (1957) 321.
[11] M. Smialowski, 'Hydrogen in steel', Pergamon Press, London, (1962).
[12] S. Venkatesan, R. Subramanian and M. A. V. Devanathan, *Met. Finish.* **64** (1966) 50.
[13] S. Venkatesan and S. K. Rangarajan, *ibid.* **69** (1971) 32.
[14] W. Paatsch, Extended Abst., ISE 30th Meeting (1979) p. 310.
[15] S. D. Bagev, *Soviet Electrochem.* **18** (1982) 1294.
[16] K. Balakrishnan and G. Devarajan, Proceedings of the 2nd International Symposium on Industry and Oriented Electrochem, Society for the Advancement of Electrochemical Science and Technology, Karaikudi (1980) 62.
[17] N. V. Parthasarathy, Ph.D. thesis, Banaras Hindu University (1981).
[18] N. J. Paul, G. Prasanna Kumar and H. V. K. Udupa, *Met. Finish.* **72** (1974) 36.
[19] T. K. G. Namboodiri and L. Nanis, *Acta Metall.* **21** (1973) 663.
[20] P. K. Subramanian, Ph.D. thesis, Pennsylvania University (1976).
[21] S. S. Chatterjee, B. G. Ateya and H. W. Pickering, Naval Research, Tech. Report No. 8, Pennsylvania University (1977).
[22] *Idem, Met. Trans.* **A9** (1978), 389–95.
[23] R. N. Iyer, I. Takeuchi, M. Zamanzadeh and H. W. Pickering, *Corrosion*, **46**(6) (1990) 460–8.